Lawrence Berkeley National Laboratory

Lawrence Berkeley National Laboratory

Title

Proton transfer in nucleobases is mediated by water

Permalink

https://escholarship.org/uc/item/3s93c8s1

Author

Khistyaev, Kirill

Publication Date

2013-07-19

eScholarship.org Powered by the California Digital Library
University of California

Proton transfer in nucleobases is mediated by water

Kirill Khistyaev[1], Amir Golan[2], Ksenia B. Bravaya[1],
Natalie Orms[1], Anna I. Krylov[1], and Musahid Ahmed[2]
[1] Department of Chemistry, University of Southern California,
Los Angeles, CA 90089-0482, USA
[2] Chemical Sciences Division, Lawrence Berkeley National Laboratory, Berkeley , CA 94720, USA

Water plays a central role in chemistry and biology by mediating the interactions between molecules, altering energy levels of solvated species, modifying potential energy profiles along reaction coordinates, and facilitating efficient proton transport through ion channels and interfaces. This study investigates proton transfer in a model system comprising dry and microhydrated clusters of nucleobases. With mass spectrometry and tunable vacuum ultraviolet (VUV) synchrotron radiation, we show that water shuts down ionization-induced proton transfer between nucleobases, which is very efficient in dry clusters. Instead, a new pathway opens up in which protonated nucleobases are generated by proton transfer from the ionized water molecule and elimination of a hydroxyl radical. Electronic structure calculations reveal that the shape of the potential energy profile along the proton transfer coordinate depends strongly on the character of the molecular orbital from which the electron is removed, i.e., the proton transfer from water to nucleobases is barrierless when an ionized state localized on water is accessed. The computed energetics of proton transfer is in excellent agreement with the experimental appearance energies. Possible adiabatic passage on the ground electronic state of the ionized system, while energetically accessible at lower energies, is not efficient. Thus, proton transfer is controlled electronically, by the character of the ionized state, rather than statistically, by simple energy considerations.

Excited-state proton transfer (PT) is ubiquitous in chemistry [1–3] and biology, occurring, for example, in photoactive proteins such as green fluorescent [4] and photoactive yellow proteins [5]. In DNA, excited-state proton transfer between the nucleobases is a pathway contributing to photoprotection[6, 7]. The driving force for excited-state proton transfer in

DNA is the increased acidity of electronically excited nucleobases. Likewise, oxidized nucleobases, in which a valence electron is completely removed, also exhibit enhanced acidity leading to PT between the strands of DNA[7] and competes with electron hole (positive charge) migration along the strands[8]. Studies of isolated model systems, such as clusters of nucleobases[9, 10], reveal that ionization-induced PT is very facile, even in systems with no h-bonds such as the methylated π-stacked uracil dimer[10]. Electronic structure calculations show that ionization-induced PT between nucleobases is endothermic in the neutral ground state (e.g., 0.8 eV uphill in AT), while it is exothermic in ionized species by 0.4-0.8 eV. Furthermore, ionization-induced PT in h-bonded pairs is barrierless suggesting a high efficiency for this process. Interestingly, even in π-stacked systems that have no h-bonds, PT is only slightly endothermic and involves a moderate barrier (0.2 eV in methylated uracil dimer); consequently, this channel opens up very close to the ionization threshold. A very recent study[11] of one-electron oxidation of DNA in solution has found that the initial steps involve proton transfer from a methyl group of thymine; thus, providing experimental evidence of the facile PT from non-hydrogen bonded moieties in realistic environments.

Water is believed to be instrumental for PT in biological systems[12], such as in water-filled ion channels, as well as through interfaces, membranes and in aerosols[13]. The ability of water to form so-called "water wires" facilitating a relay-type transport of protons, the Grotthuss mechanism, is essential in all these processes[14, 15]. The proton-coupled electron transfer in DNA also involves water wires[11]. Notwithstanding the importance of water-mediated ground- and excited-state PT, these processes are not well understood, and only a few studies have emerged to shed light on the underlying mechanistic details and dynamics. For example, a recent study of small $NO^+(H_2O)_n$ clusters investigated how the shape of h-bonded network controls proton-coupled water activation in HONO formation in the ionosphere [16]. Sequential PT through water bridges in acid-base reactions has been studied by time-resolved experiments in which the reaction has been initiated by an optical trigger exciting the photoacid[17]. Resonant ionization spectroscopy of gas-phase h-bonded clusters was employed to investigate proton versus hydrogen transfer pathways[18]. Various experimental techniques, most notably ion based infrared spectroscopy, have been used to quantify important energetics and dynamics of ionization-induced PT, and the catalytic action of solvating waters on tautomerization equilibria via PT[19–22]. However a detailed understanding of the reaction pathways and directionality of PT in model systems, let alone

in real biological and chemical systems remains elusive.

In this article, we report that water has a dramatic effect on the PT in ionized species. We focus on methylated uracil clusters, capitalizing on our previous experience with this model system and absence of low energy tautomers[10, 23]; however, similar effects were also observed in microhydrated thymine species. We consider 1,3-dimethyluracil (mU, structure shown in Fig. 1)and its deuterated analog, d6-1,3-dimethyluracil (DmU). Mass spectrometry coupled with tunable VUV radiation molecular beam experiments show that microhydration changes the branching ratio between different relaxation channels and entirely shuts down PT between the bases. Instead, a new pathway opens up, where protonated nucleobases are produced via PT from the ionized water molecule and elimination of the hydroxyl radical. Electronic structure calculations reveal that the shape of the potential energy profile along the PT coordinate depends strongly on the character of the molecular orbital from which the electron is removed, i.e., the PT from water to nucleobases becomes barrierless upon access of an ionized state localized on water. The computed energetics of PT is in excellent agreement with the experimental appearance energies. We also note that the possible adiabatic processes, which become energetically accessible at lower energies, are not efficient. Thus, PT is controlled electronically, by the character of the ionized state, rather than statistically, by simple energy considerations.

The experiments were performed on a molecular beam apparatus[24] on the Chemical Dynamics Beamline at the Advanced Light Source (Fig. S1 SM). A judicious combination of experimental source conditions (backing pressure and reservoir heater temperature) allowed us to vary the population of dimethyl uracil monomers, dimers, and their microhydrated clusters with up to 7 water molecules in the molecular beam (Fig. S2 SM). The origin of transferred proton is determined by using various combinations of deuterated and non-deuterated species, such as DmU-H_2O versus mU-D_2O.

The structures of the representative isomers of mU and its dimer hydrated with one or two water molecules are shown in Fig. 1. Because of methylation, only uracil's oxygens, O(mU) are available for h-bonding. Consequently, in mono-hydrated structures, water acts as a proton donor. The H(H_2O)...O(mU) bond length are 1.87 Å and 1.80 Å in mU-H_2O and $(mU)_2$-H_2O, respectively. The second water molecule forms an h-bond with the first water molecule in mU-$(H_2O)_2$. In hydrated $(mU)_2$, the second water forms an h-bond with the second uracil ring.

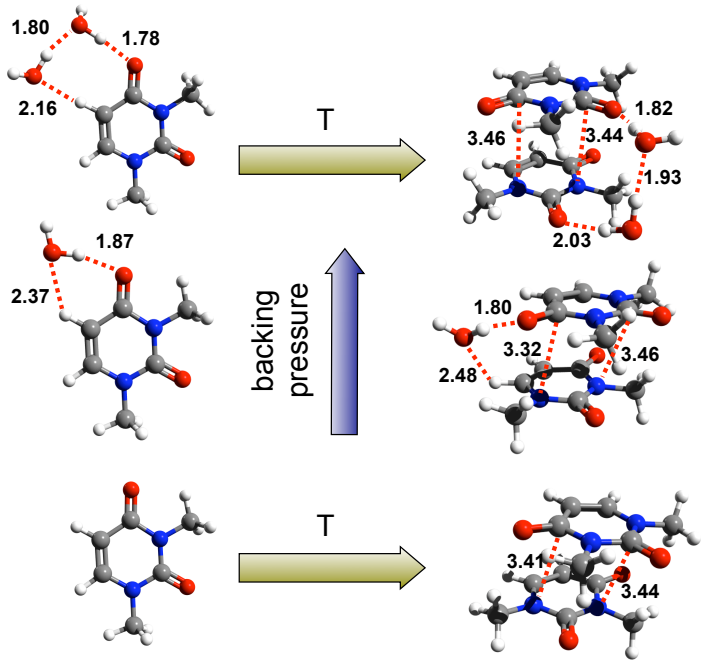

FIG. 1: Structures of 1,3-dimethyluracil and its dimer hydrated with one or two water molecules. In all structures, water acts as a proton donor. Hydration of the dimer does not lead to considerable changes in the relative position of the two mU moieties, e.g., the distances between C=O and C-CH_3 groups in dry and hydrated $(mU)_2$ clusters are around 3.3-3.5 Å. Temperature increase results in higher concentration of mU clusters, whereas backing pressure controls degree of hydration.

Previously[10], we demonstrated that PT between the bases in mU dimers occurs from a methyl group. Thus, the following PT reactions are possible in ionized $(mU)_2(D_2O)$ clusters:

$$(mU)_2(D_2O)^+ \rightarrow (mU)_2D^+ + OD \rightarrow mUD^+ + mU + OD \quad (1)$$

$$(mU)_2(D_2O)^+ \rightarrow (mU)_2H^+ + D_2O \rightarrow mUH^+ + mU + D_2O \quad (2)$$

Likewise, in $(mU)_n(D_2O)_m$ clusters, the appearance of protonated species is due to the PT between the bases, whereas the deuteron transfer will signify PT from the solvent to uracil. By considering the ratios of the respective m/z peaks, one can quantify the efficiency of these competing PT channels.

Fig. 2A shows a VUV single photon ionization mass spectrum of the molecular beam with ion signals corresponding to the mU monomer (at m/z 140), dimer (at m/z 280), and their clusters with D_2O. The inset in Fig. 2A shows an enlarged portion of the spectrum around m/z 180 where the main feature corresponds to the $mU(D_2O)_2$ ion, a cluster of

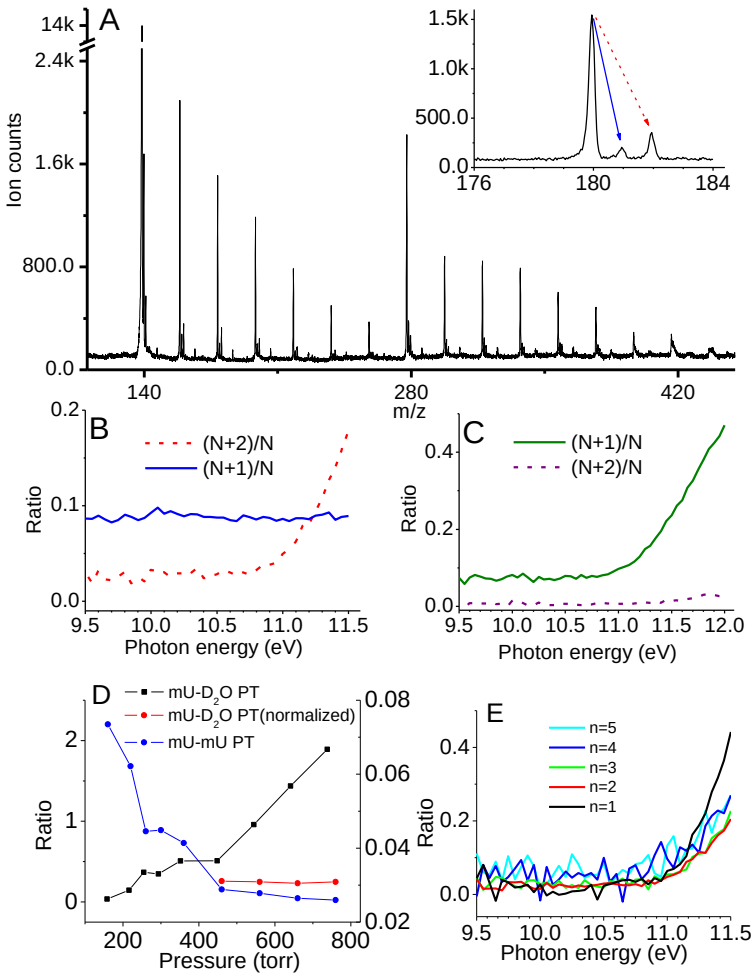

FIG. 2: Mass spectrum of hydrated mU and the dependence of the yield of various protonated species on photon energy and backing pressure. A. Mass spectrum of hydrated (with D_2O) mU and its dimer using 12 eV photons. The inset shows the region at mass to charge (m/z) 180 corresponding to $[mU(D_2O)_2]^+$. The dashed lines indicate two additional peaks at m/z 181 and 182 arising due to natural isotope abundance (^{13}C) and due to protonated and deuterated species. The intensity ratios between the peaks marked by the arrows at different photon energy for $mU(D_2O)_2$ are shown in panel B. The constant behavior of the m/z 181 peak confirms that it arises from isotopic contributions and is not due to PT. Panel C shows similar ratios (for N+1 and N+2 m/z peaks) for N=182 corresponding to $[DmU(H_2O)_2]^+$. In this case, the N+2 peak is constant, revealing that there is no deuteron transfer between the bases. Panel D: The effect of backing pressure (Ar gas) on PT. The black curve (mU-D_2O PT) characterizes deuteron transfer from D_2O to uracil; the red curve [mU-D_2O PT (normalized)] — deuteron transfer from D_2O to uracil divided by the sum of mU and $(mU)_2$ hydrates, $\sum_{n,m}[(mU)_n(D_2O)_mD]^+/\sum_{n,m\neq 0}\sum_{k+l=0,1}[(mU)_n(D_2O)_mH_kD_l]^+$. The blue curve (mU-mU PT) corresponds to PT between the mU molecules, $\sum_n[mU(D_2O)_nH]^+/\sum_m[(mU)_2(D_2O)_m]^+$. E: The appearance energies of deuterated species $[mU(D_2O)_nD]^+$ for different cluster sizes n.

one mU and two deuterated waters. The two adjacent smaller peaks (at m/z N+1 and

N+2, marked by solid and dashed arrows, respectively, where N=180) arise either due to the natural isotope abundance (^{13}C) or from protonated/deuterated species. As discussed below, similar spectra were obtained for the DmU-H_2O mixture. The isotopes account for 7.5 % and 1 % of the peaks at m/z 181 and m/z 182, respectively; similar values are obtained for the other hydrated species (SM). Contrary to the PT yield, the natural isotope contributions do not depend on the photon energies, thus, the energy dependence of the ratio between N+1 and N+2 peaks to the parent peak [N=180 for mU$(D_2O)_2$ or N=182 for DmU$(H_2O)_2$] allows us to distinguish between proton/deuterium transfer versus natural isotopes. As illustrated in Fig. 2B, the (N+1)/N ratio (solid line) is constant in the mU-D_2O beam, whereas the (N+2)/N (dashed line) exhibits a clear onset (followed by a sharp rise) at about 10.8 eV. This demonstrates that there is no PT between the bases; rather, there is a deuterium transfer from the solvating D_2O to the mU dimer.

To confirm that the proton/deuterium transfer can only occur from the solvent, we repeated the experiment with DmU and non-deuterated water (H_2O). Fig. 2C shows (N+1)/N and (N+2)/N ratios (solid and dashed lines, respectively) for N=182, which corresponds to the DmU$(H_2O)_2$ cation. Here we observe that the N+1 peak (proton transfer) exhibits a threshold behavior (at 10.8 eV, as in the mU-D_2O experiments, Fig. 2B), while (N+2)/N remains constant. Thus, there is no deuterium transfer between the DmU species. Note, that the kinetic isotope effect on the inter-base PT was found to be minor for the stacked mU dimer [10], and, therefore, the constant behavior of the (N+2)/N peak in the DmU-H_2O is not due to H/D exchange in the base. Essentially water shuts down PT between the mU bases, which opens up at 8.9 eV in the absence of water[10].

In Fig. 2A, there is evidence of mU dimers in the molecular beam. Furthermore, we can control the degree of dimerization relative to solvation by varying the backing pressure of the carrier gas (Ar), as illustrated in Fig. S2 (SM).

Fig. 2D shows the effect of backing pressure on the relative efficiency of PT in the mU-D_2O beam. The increase of backing pressure increases the yield of hydrated species, at the expense of bare mU dimer and monomer. However the total amount of all forms of the mU dimers (bare dimer plus all hydrated dimers) remains roughly the same (Fig. S3).The yield of interfragment PT is given by the signal of all protonated species (dominated by mUH^+, more than 85%). When normalized to the total dimer population, the yield of protonated species decreases with backing pressure (Fig. 2D mU-mU PT blue curve). This suggests that the

interfragment PT is suppressed by hydration of dimers rather than reducing the population of dimers via monomer hydration (hence reducing the number of molecules available for clustering). The yield of all deuterated forms of mU increases upon hydration, as shown by the ratio of all deuterated forms to all forms of mU present in the beam (black line). Finally, upon normalization to the population of the hydrated species, we observe a constant ratio of all deuterated forms to all hydrated forms of mU (mU-D_2O (normalized) red line around 0.25), hence confirming that the increased yield of PT is proportional to the degree of hydration. This suggests that the rate of PT in the hydrated clusters (and, possibly, its mechanism) does not depend on degree of hydration.

To understand the mechanism by which water shuts down PT between the bases, we turn to electronic structure calculations. Previous theoretical studies of microhydrated nucleobases[25] reported a small red-shift ($\sim$ 0.4 eV) in the lowest IE, in excellent agreement with experiments[20, 25]. The calculations revealed that the character of the ionized state remains the same as in the isolated base (π_{CC} orbital); the red-shift was explained by the fact that in the lowest-energy microhydrated structures, the nucleobase is acting as a proton donor. Using similar computational protocols (see SM), we conducted electronic structure calculations of micro-hydrated mU dimers.

We observe that the hydration by one or two water molecules does not change the relative distance between the two mU moieties (see Fig. 1), e.g., the distance between C(=O) and C(-CH_3) moieties, which are involved in inter-base PT, in the mU dimer is 3.4 Å, whereas in $(mU)_2(H_2O)$ and $(mU)_2(H_2O)_2$ it varies between 3.3-3.5 Å.

The effect on the lowest ionized state is small, both in terms of energy and the character of the state. We observe a moderate blue shift ($\sim$0.1-0.3 eV) in the VIE, which is consistent with the structures of hydrated species (see Fig. 1) where uracil acts as a proton acceptor. The character of the lowest ionized state is also unaffected, as evidenced by the wave function composition and the shapes of the respective MOs (Fig. S9).

Thus, neither structure nor energetics of the lowest IE explains the observed behavior. However, we note that water blocks the proton-accepting sites in mU; it may also add structural rigidity to the system. The analysis of higher ionized states (see Table S1) reveals that while hydration has relatively small effect on the lowest ionized states of mU, the ionized states localized on water are affected much more strongly by the interaction with mU. Specifically, the state corresponding to ionization from a lone pair in water appears at

10.9-11.5 eV in mU mono- and dihydrates, which is 1-1.5 eV lower compared to the bare water monomer. The lower bound of the energy range is remarkably close to the observed onset of PT in microhydrated clusters (10.8 eV). These results suggest that the PT channel opens up when the lowest ionized state on solvated water which corresponds to an excited ionized state of the $mU(H_2O)_n$ cluster becomes accessible. These results are consistent with the experimentally observed onsets of PT, which are independent of the cluster size (see Fig. 2E), in stark contrast to the lowest IE of microhydrated nucleobases which show notable dependence on the number of hydrated waters ($\sim$ 0.1 eV drop in IE per water molecule)[20, 24, 25].

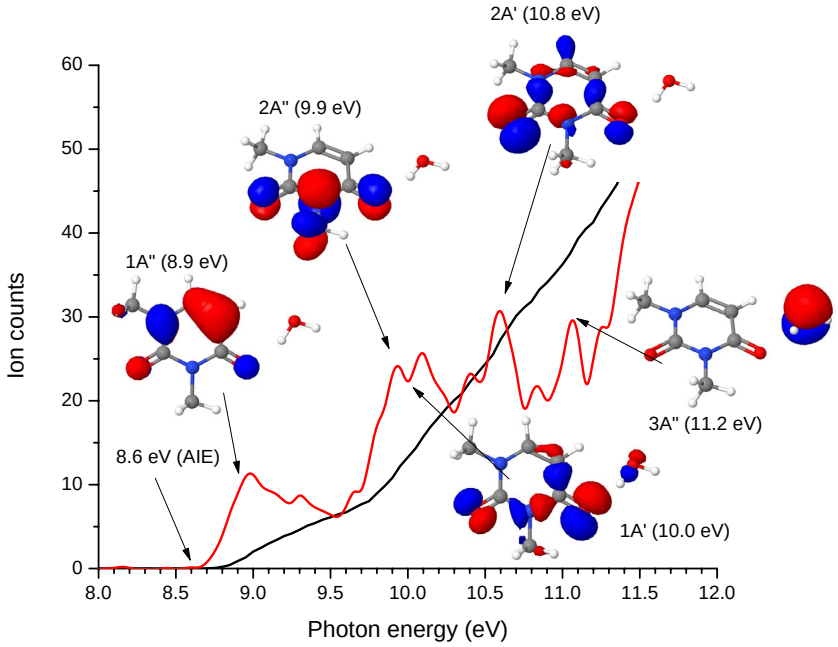

FIG. 3: Photoionization efficiency curve (black) of $[(mU+D_2O)]^+$ and its derivative (red), observed using 8 eV to 12 eV photons. The derivative plot reveals multiple ionized states derived by removing the electron from different MOs. Black arrows points towards the calculated ionization energies.

To gain further insight into the electronic structure of hydrated species and to validate theory, we focus on the photoionization efficiency (PIE) curve (obtained by integrating the area under the respective m/z peak) of the smallest hydrated cation, $mU(D_2O)$. The differentiation of the PIE curve allow identification of multiple ionized states (the peaks on the differentiated PIE curve correspond to the VIEs). The PIE (black) and the differentiated

(red) curves are shown in Fig. 3, along with the computed VIEs. The curve features the ionization onset at $\sim$ 8.6 eV and a series of peaks between 8.5 and 11.5 eV. The computed AIE is in excellent agreement with the experimental onset, whereas the computed VIEs match well the peaks of the differentiated curve. Thus, the peaks at 8.9, 9.9, 10.0, 10.8 and 11.2 eV correspond to vertical ionizations from the 1A$''$, 2A$''$, 1A$'$, 2A$'$, and 3A$''$ states, respectively. The character of these states are illustrated by the respective molecular orbitals which are also shown in Fig. 3. As Fig. 3 clearly illustrates, low-lying electronic ionized states correspond to the ionization from mU, whereas the 3A$''$ state at 11.2 eV is localized on water, and is similar to the water-localized states observed in microhydrated dimers.

To further understand PT in solvated systems, we analyze the potential energy profiles along the PT coordinate in $[mU(H_2O)]^+$. An approximate reaction coordinate was generated by the interpolation between the initial structure of the neutral $mU{\cdot}H_2O$ and that of the proton-transferred system, $mUH^+{\cdot}OH$ (see SM). The profiles are shown in Fig. 4. The energy of the ionized states that are localized on mU (1A$''$ and 2A$''$, see Fig. 3) increases along the PT coordinate (the PT is also endothermic in the neutral state). In contrast, the energy of the fifth state (3A$''$) corresponding to the ionization of water decreases showing that PT from this state is a barrierless downhill process. A similar behavior is observed for other states, in that energetically, — water-ionized states go down, whereas uracil-localized states go up. Alternatively, one can consider a possibility of adiabatic PT, e.g., on the lowest ionized state (1A$''$). This will of course involve changes in the electronic state character from the mU-localized one to the water-ionized one and a barrier. The analysis of energy profiles shows that PT is energetically accessible at $\sim$10.6 eV (upper bound), i.e., at this energy the system has enough energy to overcome the barrier on the adiabatic PES corresponding to the lowest ionized state of the system. Yet, the onset of PT yield occurs only at 10.8 eV thus suggesting that such an adiabatic process is inefficient. This can be readily rationalized by analyzing the respective electronic wave functions. The lowest ionized state corresponds to the ionization of mU, which reduces the proton affinity of mU. Hence the short-time dynamics will involve structural changes which are not favorable for PT from water. Indeed, in the Franck-Condon optimized structures of the lowest electronic state of $[mU{\cdot}H_2O]^+$ (Fig. S8) the distance between O(mU) and water hydrogen increases from 1.87 Å to 2.90 Å. In contrast, PT is barrierless starting from the Franck-Condon point in the fifth ionized state. Thus, even though the system may have enough energy to overcome the barrier on the lowest

ionized state adiabatic PES, this pathway is not favored dynamically because the gradients in the Franck-Condon region point away from the PT coordinate. In contrast, when the right electronic state is accessed, the PT may occur ballistically on the respective diabatic surface. We observe that PT in hydrated mU species is controlled electronically, by the character of the state, rather than statistically, by energy considerations alone.

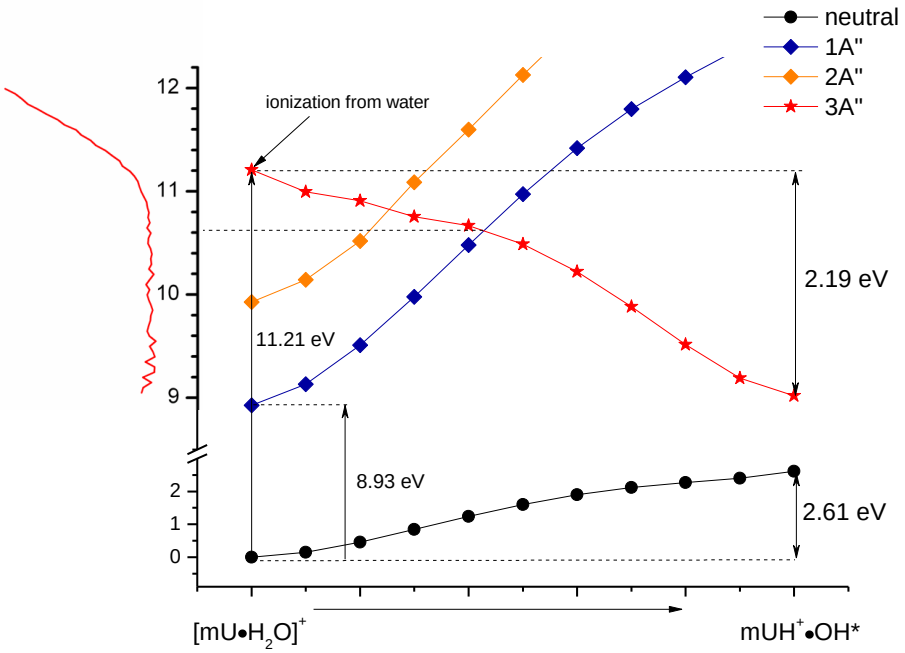

FIG. 4: Potential energy profiles for low-lying states of $[mU{\cdot}H_2O]^+$ along the PT reaction coordinate. The proton is moved from the water molecule to the mU oxygen site. The 5th ionized state, $3A''$, in which the hole is on the water molecule (see Fig. 3), shows no barrier facilitating downhill PT. PT from lower ionized states are possible, however this involves changes in the electronic wave function character and requires more than 10.6 eV photon energy. The left panel shows the experimental ratio between the $[mU(D_2O)_2]^+$ signal (m/z 180) and $[mU(D_2O)_2D]^+$ the deuterated species at m/z 182; it shows dramatic enhancement in PT when the $3A''$ state is accessed.

The appearance energies of $mU(H_2O)_nH^+$ does not depend on the cluster size, as illustrated in Fig. 2E, and to understand this, we consider a dihydrated system, $mU(H_2O)_2$ (see Fig. 1B). In this structure, the second (outer) water molecule acts as a proton donor forming an h-bond with the first (inner) water h-bonded to the carbonyl group. One can consider several possibilities for ionization-induced PT leading to: (A) a structure with H_3O^+ resulting from a single PT from the outer molecule; (B) a structure with protonated mU bound

to the OH radical and solvated by the outer water molecule derived by single PT from the inner water molecule to mU, and (C) a structure with protonated mU solvated by water and an outer OH radical.

We have found (see SM, Fig. S11) that the most energetically favorable structure is (C), which can be easily rationalized by the number of h-bonds and relative proton affinities of mU and water. The difference between structures (B) and (C) is about 23 kcal/mol. Interestingly, there is no barrier for Grotthuss-like double PT leading to structure (C). We also note that there is no local minima corresponding to the structure with H_3O^+, which can be considered as an intermediate along the double stepwise PT pathway from the outer water to uracil.

In large water clusters, the lowest ionized states correspond to the surface states, where there are waters that serve only as proton donors[26]. Thus, the IEs corresponding to the surface states should be relatively independent of the cluster size (and even the chemical nature of its core). The experimental onsets for protonated $mU(H_2O)_n$ clusters are remarkably insensitive to the cluster size (Fig. 2E); this suggest that in larger clusters the surface-ionized states lead to multiple barrierless PT yielding solvated protonated uracil with the OH radical on the surface. Thus, such clusters of water with molecules with relatively high proton affinity could serve as model systems for studying directionality in Grotthuss-like PT through water wires and membrane interfaces[27, 28].

While most of the experiments in this work focused on mU, this nucleobase is by no means unique in that water has a significant effect on PT. Similar experiments performed on thymine show that in the absence of water, PT begins at 9.20 eV, with a major rise in signal between 9.7 and 9.9 eV[9]. Thymine provides an interesting comparison, because both h-bonded and π-stacked dimers populate the molecular beam[9], in contrast to mU which forms only π-stacked dimers[10]. The calculations suggested that it is h-bonded thymine dimers which give rise to this signal at 9.7 eV, while the lower onset was explained by a dimer with π-stacked geometry[9]. Upon solvation, PT switches off at these lower energies, as is evidenced in the signal for TH^+ and $T(H_2O)H^+$ shown in Fig. S5 (SM). The onset for PT is around 10.6 eV, with a major rise at 11.2 eV, which is very similar to the onsets observed in mU. The shapes of the curves for protonated thymine species are also very similar to those in Fig. 2B and C. This suggests that a similar PT mechanism from the solvent is occurring.

We conclude that both in h-bonded and π-stacked nucleobase dimers and larger clusters,

solvation shuts down PT between the bases, which is rather efficient in "dry" clusters. It is only when the solvent is ionized that PT begins again. Our findings illustrate that water has a dramatic effect on PT pathways, not only by serving as a wire for proton transport, but also by shutting down other PT routes. In our model systems, an outermost ionized water molecule acts as an acid (activated by an ionization event), and the nucleobase — as a base, whereas other waters may participate in PT either as spectators or as intermediate proton acceptors, as shown recently in photo induced acid-base reactions[17]. We explain the remarkable similarity between the appearance onsets in solvated mU and thymine, as well as insensitivity of the onsets and shapes of the appearance curves on the cluster sizes to the fact that the lowest ionized states in which the hole is localized on the solvent correspond to the surface states, i.e., water molecules acting as proton donors only. Electronic structure calculations show that these IEs are rather insensitive to the size and/or chemical identity of the cluster core (mU versus mU dimer versus thymine). Thus, these states become accessible at very similar energies initiating facile PT to the accepting base, either directly (in monohydrates), or through the mediating water molecules.

While our study focuses on PT in a simple model system, one can anticipate that some of these mechanisms may be operational in solution or in biological environments. A growing body of studies illustrating the central role of PT has led to a paradigm shift in the discussion of water and its active role in biology and chemistry. Water is no longer seen as just a solvent, but is an active participant in a variety of processes such as enzyme catalysis and membrane transport. Water has also been shown to catalyze reactions[29] which are important in biology and atmospheric chemistry[16, 30]. Proton-coupled electron transfer in DNA is mediated by water chains[11]. Autoionization in water also drives a variety of processes which are critical to life and biology[12], while PT through nanopores, artificial membranes and structures have major ramifications in energy conversion and storage technologies. PT in nano confined geometries[31] have implications for catalysis and solar energy conversion, while ions have been shown to enhance the transfer of protons through aqueous interfaces[32]. In this work we have shown that PT can be very effectively controlled by subtly changing how DNA bases hydrogen bond and stack within themselves and upon solvation and thus can provide a template for novel dynamical studies in the temporal, spatial, and spectroscopic domain.

Acknowledgment

AG, MA and the ALS are supported by the Office of Science, Office of Basic Energy Sciences, of the US Department of Energy under Contract No. DE-AC02-05CH11231, through the Chemical Sciences Division. AIK acknowledges support from the Department of Energy through the DE-FG02-05ER15685 grant. The authors acknowledge the contributions of Oleg Kostko in providing the thymine/water data and Qiao Ruan for mass spectra analysis.

[1] A. Rosspeintner, B. Lang, and E. Vauthey, Ultrafast photochemistry in liquids, Annu. Rev. Phys. Chem. **64**, 247 (2013).

[2] L.M. Tolbert and K.M. Solntsev, Excited-state proton transfer: From constrained systems to "super" photoacids to superfast proton transfer, Acc. Chem. Res. **35**, 19 (2002).

[3] S.J. Formosinho and L.G. Arnaut, Excited-state proton transfer reactions ii. intramolecular reactions, J. Photochem. Photobiol. **75**, 21 (1992).

[4] J.J. van Thor, Photoreactions and dynamics of the green fluorecent protein, Chem. Soc. Rev. **38**, 2935 (2009).

[5] E.C. Carroll, S.-H. Song, M. Kumauchi, I.H.M. van Stokkum, A. Jailaubekov, W.D. Hoff, and D.S. Larsen, Subpicosecond excited-state proton transfer preceding isomerization during the photorecovery of photoactive yellow protein, J. Phys. Chem. Lett. **1**, 2793 (2010).

[6] T. Schultz, E. Samoylova, W. Radloff, I.V. Hertel, A.L. Sobolewski, and W. Domcke, Efficient deactivation of a model base pair via excited-state hydrogen transfer, Science **306**, 1765 (2004).

[7] A.K. Ghosh and G.B. Schuster, Role of the guanine N1 imino proton in the migration and reaction of radical cations in DNA oligomers, J. Am. Chem. Soc. **128**, 4172 (2006).

[8] T. Charkaborty, editor, *Charge Migration in DNA*. Springer, 2007.

[9] K.B. Bravaya, O. Kostko, M. Ahmed, and A.I. Krylov, The effect of π-stacking, h-bonding, and electrostatic interactions on the ionization energies of nucleic acid bases: Adenine-adenine, thymine-thymine and adenine-thymine dimers, Phys. Chem. Chem. Phys. **12**, 2292 (2010).

[10] A. Golan, K.B. Bravaya, R. Kudirka, S.R. Leone, A.I. Krylov, and M. Ahmed, Ionization of dimethyluracil dimers leads to facile proton transfer in the absence of H-bonds, Nature Chem. **4**, 323 (2012).

[11] R.N. Barnet, J. Joseph, U. Landman, and G.B. Schuster, Oxidative thymine mutation in DNA: Water-wire-mediated proton-coupled electron transfer, J. Am. Chem. Soc. **135**, 3904 (2013).

[12] P. Ball, The importance of water, in *Astrochemistry and Astrobiology*, edited by I.W. M. Smith, C.S. Cockell, and S. Leach, Physical Chemistry in Action, pages 169–210. Springer Berlin Heidelberg, 2013.

[13] G.A. Voth, Computer simulation of proton solvation and transport in aqueous and biomolec-

ular systems, Acc. Chem. Res. **39**, 143 (2006).

[14] C.J.T. de Grotthuss, The Grotthuss mechanism, Chem. Phys. Lett. **244**, 456 (1995).

[15] D. Chandler, C. Dellago, and P. Geissler, Wired-up water, Nat. Chem. **4**, 245 (2012).

[16] R.A. Relph, T.L. Guasco, B.M. Elliott, M.Z. Kamrath, A.B. McCoy, R.P. Steele, D.P. Schofield, K.D. Jordan, A.A. Viggiano, E.E. Ferguson, and M.A. Johnson, How the shape of an h-bonded network controls proton-coupled water activation in HONO formation, Science **327**, 308 (2010).

[17] O.F. Mohammed, D. Pines, J. Dreyer, E. Pines, and E.T.J. Nibbering, Sequential proton transfer through water bridges in acid-base reactions, Science **310**, 83 (2005).

[18] C. Manca, C. Tanner, and S. Leutwyler, Excited state hydrogen atom transfer in ammonia-wire and water-wire clusters, Int. Rev. Phys. Chem. **24**, 457 (2005).

[19] L. F. Sukhodub, Interactions and hydration of nucleic acid bases in a vacuum. experimental study, Chem. Rev. **87**, 589 (1987).

[20] S.K. Kim, W. Lee, and D.R. Herschbach, Cluster beam chemistry: Hydration of nucleic acid bases; Ionization potentials of hydrated adenine and thymine, J. Phys. Chem. **100**, 7933 (1996).

[21] N.J. Kim, H.M. Kim, and S.K. Kim, Ionization-induced proton transfer in thymineammonia van der Waals clusters, Int. J. Mass. Spectr. **261**, 32 (2007).

[22] K. Mizuse, J.-L. Kuo, and A. Fujii, Structural trends of ionized water networks: Infrared spectroscopy of water cluster radical cations $(H_2O)n^+$ (n=3-11), Chem. Science **2**, 868 (2011).

[23] A.A. Zadorozhnaya and A.I. Krylov, Zooming into pi-stacked manifolds of nucleobases: Ionized states of dimethylated uracil dimers, J. Phys. Chem. A **114**, 2001 (2010).

[24] L. Belau, K.R. Wilson, S.R. Leone, and M. Ahmed, Vacuum-ultravioled photoionization studies of the microhydration of DNA bases (guanine, cytosine, adenine, and thymine), J. Phys. Chem. A **111**, 7562 (2007).

[25] K. Khistyaev, K.B. Bravaya, E. Kamarchik, O. Kostko M. Ahmed, and A.I. Krylov, The effect of microhydration on ionization energies of thymine, Faraday Discuss. **150**, 313 (2011).

[26] P.A. Pieniazek, E.J. Sundstrom, S.E. Bradforth, and A.I. Krylov, The degree of initial hole localization/delocalization in ionized water clusters, J. Phys. Chem. A **113**, 4423 (2009).

[27] A. Springer, V. Hagen, D.A. Cherepanov, Y.N. Antonenko, and P. Pohl, Protons migrate along interfacial water without significant contributions from jumps between ionizable groups

on the membrane surface, Proc. Nat. Acad. Sci. **108**, 14461 (2011).

[28] O.-H. Kwon and O.F. Mohammed, Water-wire catalysis in photoinduced acid-base reactions, Phys. Chem. Chem. Phys. **14**, 8974 (2012).

[29] Y. Matsuda, A. Yamada, K. i. Hanaue, N. Mikami, and A. Fujii, Catalytic action of a single water molecule in a proton-migration reaction, Angew. Chem. Int. Ed. Engl. **49**, 4898 (2010).

[30] R.J. Buszek, J.R Barker, and J.S. Francisco, Water effect on the OH + HCl reaction, J. Phys. Chem. A **116**, 4712 (2012).

[31] J. Kofinger, G. Hummer, and C. Dellago, Single-file water in nanopores, Phys. Chem. Chem. Phys. **13**, 15403 (2011).

[32] H. Mishra, S. Enami, R.J. Nielsen, M.R. Hoffmann, W.A Goddard, and A.J. Colussi, Anions dramatically enhance proton transfer through aqueous interfaces, Proc. Nat. Acad. Sci. **109**, 10228 (2012).

This document was prepared as an account of work sponsored by the United States Government. While this document is believed to contain correct information, neither the United States Government nor any agency thereof, nor the Regents of the University of California, nor any of their employees, makes any warranty, express or implied, or assumes any legal responsibility for the accuracy, completeness, or usefulness of any information, apparatus, product, or process disclosed, or represents that its use would not infringe privately owned rights. Reference herein to any specific commercial product, process, or service by its trade name, trademark, manufacturer, or otherwise, does not necessarily constitute or imply its endorsement, recommendation, or favoring by the United States Government or any agency thereof, or the Regents of the University of California. The views and opinions of authors expressed herein do not necessarily state or reflect those of the United States Government or any agency thereof or the Regents of the University of California.